Zero Group Velocity Mode Enhanced Electro-Mechanical Impedance Spectroscopy and Nonlinear Ultrasonics

Runye Lu[1, a] and Yanfeng Shen[1,b *]

[1]University of Michigan-Shanghai Jiao Tong University Joint Institute,

Shanghai Jiao Tong University, Shanghai, 200240, China

[a]runye.lu@sjtu.edu.cn [b]yanfeng.shen@sjtu.edu.cn

Keywords: structural health monitoring; electro-mechanical impedance spectroscopy; zero group velocity mode; local resonances; nonlinear ultrasonics

Abstract. The zero group velocity (ZGV) mode possesses the distinctive attribute of an elapsed group velocity with a finite wavenumber, indicating a spatially propagating wave under a motionless package. This stationary mode engenders a localized resonance, confining the wave energy in the vicinity of actuation. Researchers have utilized ZGV modes for structural health monitoring (SHM) scenarios mostly in transient analysis and linear ultrasonic regime. Nevertheless, it remains an uncharted frontier that how ZGV mode, especially via its peculiar characteristics, can empower SHM methodologies regarding harmonics analysis and nonlinear ultrasonics. Therefore, this paper, on one hand, explores the trembling feature of ZGV resonances in steady-state electro-mechanical impedance spectroscopy (EMIS) and utilizes it for structural sensing. On the other hand, this paper leverage nonlinear generation of ZGV modes to amplify the higher harmonics signal to enhance conventional nonlinear ultrasonic methodology. This paper culminates in summary, concluding remarks, and suggestions for future work.

Introduction

The zero group velocity (ZGV) mode, as a peculiar non-propagating Lamb wave mode, has ignited enormous research interests. ZGV modes are endowed with special characteristics of a vanishing group velocity and simultaneously a non-zero phase velocity, resulting in a spatially propagating phase information under a motionless wave package [1]. Such a stationary mode can trigger intense local resonances in the thickness direction, confining the wave energy within the vicinity of the actuation site [2, 3].

The existence of ZGV modes has been validated in thin plates and membranes [1, 4-8], thin films [9], isotropic [10]/hollow cylinders [11], rigid/soft strips [12], concrete materials [13], and multi-layered structures [14, 15]. Furthermore, Li et al. validated the presence of ZGV features in a welded joint subjected to a force source [16]. Zhu et al. demonstrated the ZGV modes in free rails by numerical modelling and experimental verification [17]. ZGV modes have also been applied for various structural health monitoring (SHM) purposes. The potential application of ZGV modes for material properties determination were demonstrated, encompassing elastic constant [18], Poisson's ratio [19], interfacial stiffness [5], and bulk acoustic wave velocity [20]. Regarding various damage types, the ZGV modes enabled the diagnosis of fatigue damage [8], laminate disbond [14], delamination in composites [13]. To sum, the current SHM techinques mostly rely on the direct use of ZGV modes in transient analyses and linear ultrasonic regimes. It still remains an uncharted frontier that how ZGV resonances manifest themselves in steady-state harmonic anlaysis and whether ZGV modes can be utlized for nonlinear ultrasonics. It is worth mentioning

that the research on nonlinear generation of ZGV modes have been pioneered by Li et al. and Mora et al. [21, 22].

The paper commences with the identification and extraction of ZGV modes in aluminum plate by analytical modelling, obtaining the ZGV frequencies as references. Following this, the paper delves into the trembling feature following the ZGV resonant peaks in steady-state frequency spectra. The mechanism and nature behind the trembling features are investigated from various aspects. Subsequently, such feature is leveraged for the efficient ZGV identification and structural sensing in harmonic analysis. When it comes to the nonlinear ultrasonics, the paper conducts the comparative finite element analyses to demonstrate the enhancement performance of ZGV modes. Different from the normal frequency actuation, a half ZGV frequency actuation is employed so that the second harmonics component, which is exactly the ZGV frequency, can be generated at the fatigue crack location. The nonlinear ZGV generation triggers local resonance and thus intensive interactions, therefore enhancing the second harmonic spectral amplitude. Afterwards, some bizarre phenomena accompanying the nonlinear ZGV generation are explored and elucidated. This paper culminates in summary, concluding remarks and suggestions for future work.

Analytical Investigation on ZGV Modes in Al Plates

This section conducts the analytical investigation on the ZGV mode frequencies in the target aluminum plate as depicted in Figure 1. The dispersion curve of the aluminum plate can be obtained by solving the Rayleigh Lamb equation as depicted below:

$$\frac{\tan \eta_P d}{\tan \eta_S d} = - \left[\frac{\left(\xi^2 - \eta_S^2\right)^2}{4\xi^2 \eta_P \eta_S} \right]^{\pm 1} \tag{1}$$

where d denotes the half plate thickness; $\eta_P^2 = \omega^2 / c_P^2 - \xi^2, \eta_S^2 = \omega^2 / c_S^2 - \xi^2$; ξ signifies the wavenumber; the power of +1 refers to symmetric modes, while -1 corresponds to anti-symmetric modes. Numerical solution of Rayleigh-Lamb equation yields the eigenvalues, $\xi_0^S, \xi_1^S, \xi_2^S, ..., \xi_0^A, \xi_1^A, \xi_2^A, ...$, representing the wavenumbers of the lamb wave modes. The relationship $c = \omega / \xi$ engenders the dispersive phase velocity, as a function of the the frequency and half thickness product, fd. At a given fd product, several modes exist simultaneously, designating the multimodal feature of Lamb waves.

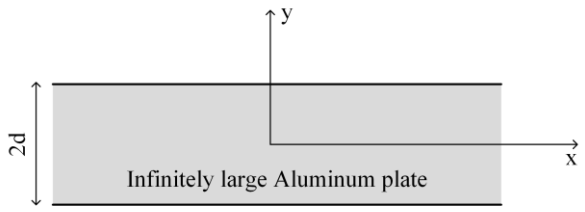

Figure 1: Diagram of the target infinitely large aluminum plate.

The aluminum plates to be utilized in the following sections take 4 mm and 1 mm in thickness respectively. The dispersion curves of the two target Al plates and the corresponding S_1-ZGV mode shape are displayed in Figure 2. The ZGV frequencies can be determined to be 707 kHz and 2828 kHz by tracing the points with zero slope in dispersion curves. The ZGV frequencies function as the reference frequency for the subsequent analyses on the two ZGV enhanced SHM methodologies.

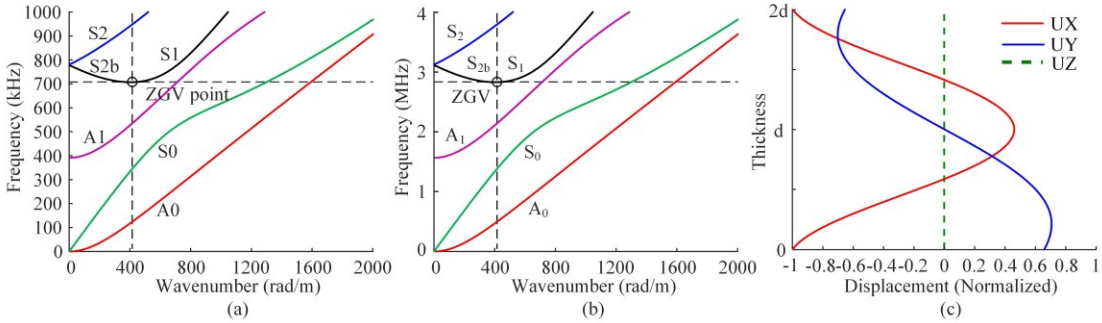

Figure 2: dispersion curves for (a) 4 mm Al plate; (b) 1 mm Al plate; (c) S_1-ZGV mode shape

Trembling Features Following ZGV Resonances in EMIS Framework

This section presents the FE analyses and experimental verification of the distinctive trembling features following ZGV resonances and corresponding application for structural sensing. The target structure is a 4 mm thick aluminum plate, the FE model of which is displayed in Figure 3. A piezoelectric wafer active sensor (PWAS) was bonded on the top center of the plate, implemented by the 2-D multi-physics element. The 100 mm non-reflective boundary at both sides was achieved by absorbing layers with increasing damping to simulate the infinitely large structure. The harmonic analysis was conducted with the frequency sweeping from 700 kHz to 720 kHz. The steady-state displacement frequency spectra were to be captured at all points in the sampling region with a spatial resolution of 0.25 mm.

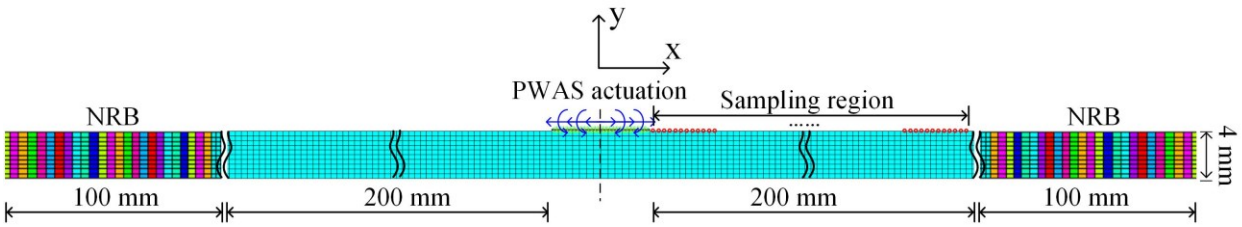

Figure 3: The FE model under EMIS configuration.

The steady-state displacement frequency spectrum captured at the first sampling point was illustrated in Figure 4. The steep ZGV resonance peak at 707 kHz can be obviously observed. The intriguing trembling features appeared right after the resonant peak and gradually faded away with the frequency increasing, akin to the accompanying local resonances.

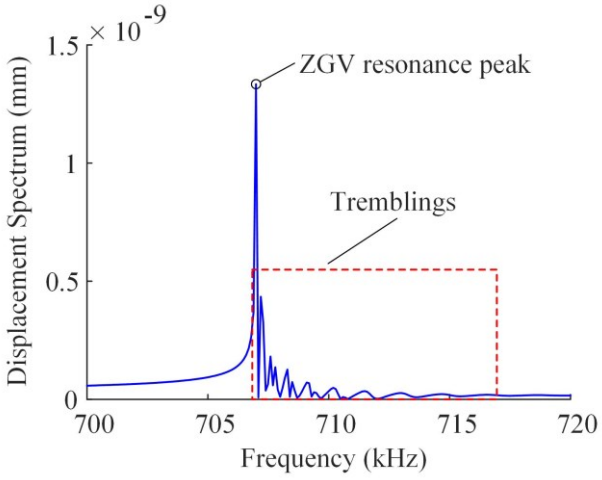

Figure 4: The steady-state displacement frequency spectrum manifesting trembling features.

Afterwards, the ZGV resonances and the trembling features were examined in frequency-wavenumber domain. Since the steady-state frequency spectra were obtained, only 1-D Fast Fourier Transformation (FFT) was required to calculate the dispersion curves. It is worth mentioning that the dispersion curves obtained here were steady-state dispersion curve, different from the conventional dispersion curves implemented by 2-D FFT from transient analysis as illustrated in Figure 5.

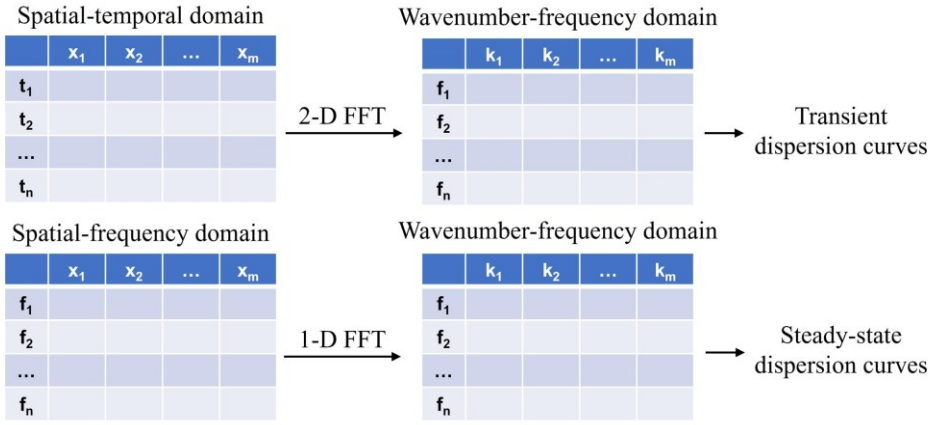

Figure 5: Comparison on the signal processing procedures.

The steady-state dispersion curve and the corresponding 3-D version were displayed in Figure 6. The dispersion curves clearly illustrated the existence of ZGV resonance occurring at 707 kHz and the alternatively dark-shallow color indicated the trembling features right after the ZGV frequency. The 3-D surface plots in Figure 6 elucidated the alternating peaks and valleys of the subsequent resonances more clearly. That is to say, following the generation of ZGV resonance, the participation level of each mode revealed drastic fluctuations and gradually settled down.

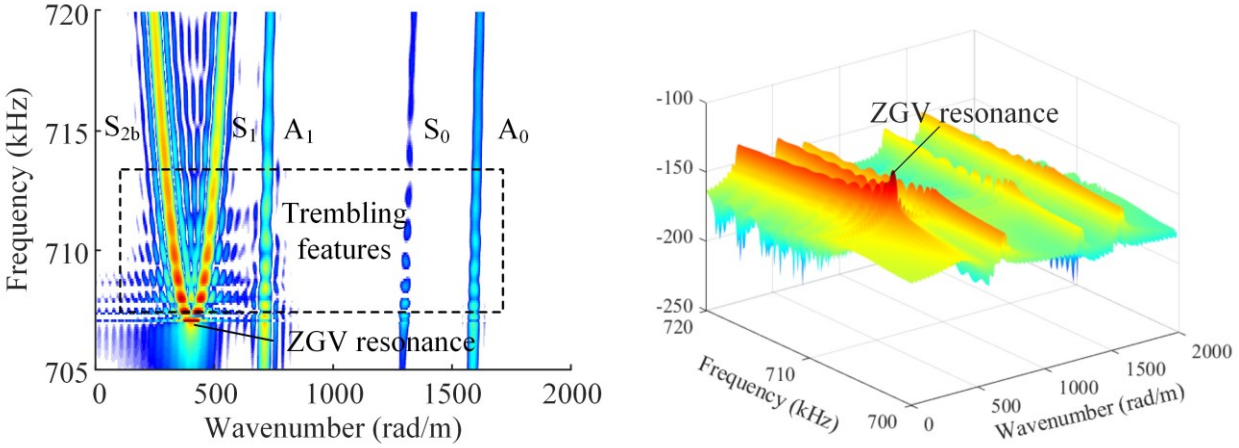

Figure 6: Steady-state dispersion curves ellucidating ZGV resonance and trembling features.

Furthermore, the distinctive trembling features were utilized for structural sensing via electromechanical impedance spectroscopy (EMIS), targeting at the multi-layer aluminum laminate. As depicted in Figure 7(a), the laminate was composed of two aluminum plates (4 mm and 6 mm in thickness) bonded by the epoxy adhesive layer. A PWAS was mounted at the top center of the plate, functioning as both the actuator and receiver. Similarly, NRB was utilized to simulate the infinitely large structure. The EMI spectrum was obtained and displayed in Figure

7(b), where the ZGV resonances were identified and extracted by the unique trembling features. The group velocity dispersion curve further validated the observation.

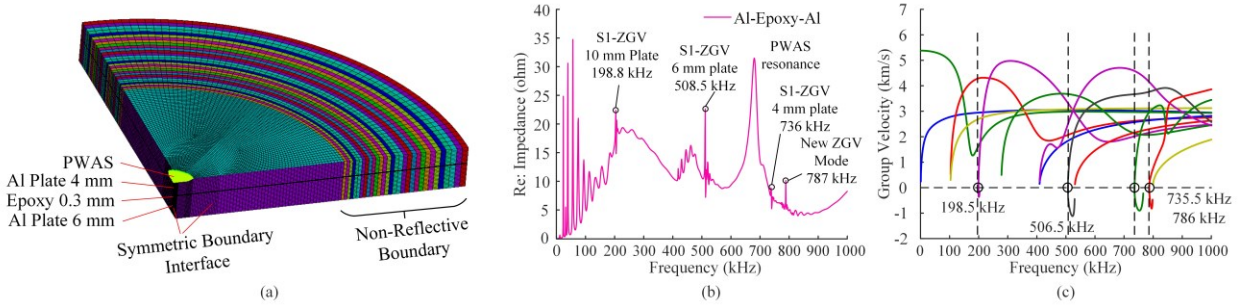

Figure 7: Structural sensing application on Al laminate (a) FE model configuraion; (b) electromechanical impedance spectra; (c) frequency-wavenumber dispersion curves.

ZGV Resonance Enhanced Nonlinear Ultrasonics for Fatigue Crack Monitoring

This section conducts comparative finite element (FE) analyses on the ZGV enhanced nonlinear ultrasonic method. The FE model of the 1 mm thick Al plate is displayed in Figure 8. The symmetric pin-force actuation was applied to output the tone burst signal at certain frequencies. The non-reflective boundaries (NRB) were employed to absorb the wave reflections to simulate the infinitely large structure. The fatigue crack was simulated by the contact element to integrate the contact acoustic nonlinearity (CAN) effect. The actuation frequencies were determined to be 1000 kHz and 1383 kHz, corresponding to normal excitation and half ZGV frequency (2776 kHz /2) excitation respectively. The temporal displacement responses of the sampling points in the denoted sampling region were captured.

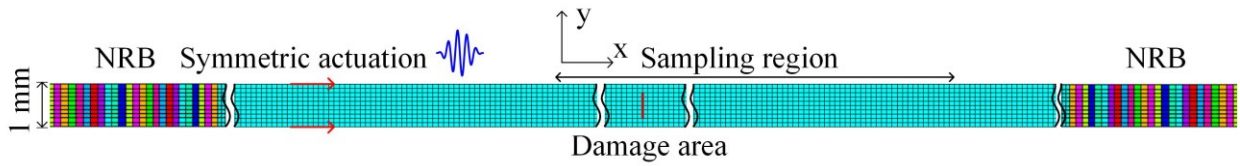

Figure 8: FE model configurations for the ZGV enhanced nonlinear ultrasonic method.

The temporal domain displacement responses three points (0 mm, 5 mm, 10 mm at the surface) are displayed in Figure 9. The displacement amplitude of the half ZGV actuation overwhelms the normal frequency actuation and the ringing effect of the ZGV mode with a longer time duration is observed.

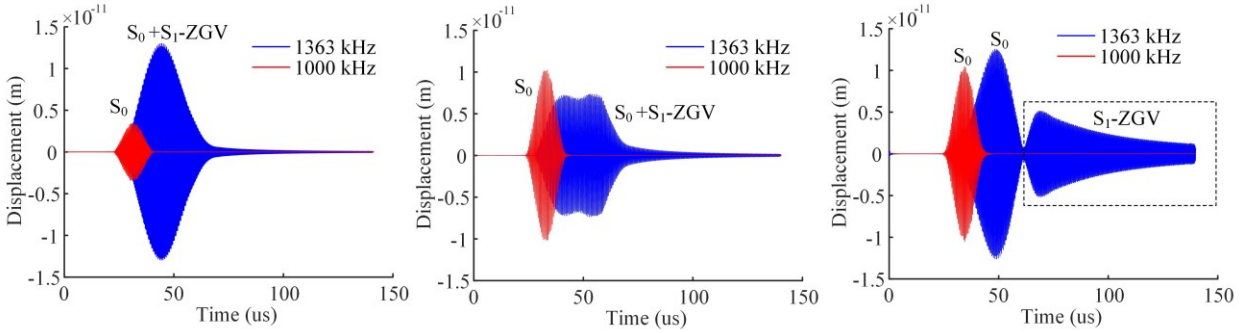

Figure 9: Temporal displacement responses for the two actuation frequencies at three selective points.

Afterwards, FFT was applied on the temporal signal at the point top of the crack to obtain the frequency spectra as depicted in Figure 10. The results from the half ZGV excitation manifested a drastic amplification of the second harmonic component, even larger than the fundamental frequency component. Following the frequency spectra, 2-D FFT was implemented on the signals at all sampling points to obtain the frequency-wavenumber dispersion curves as showcased in Figure 11. The nonlinear ZGV generation can be further validated via the partially marked curves.

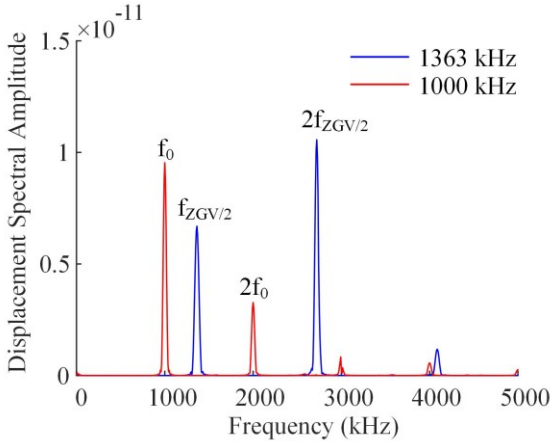

Figure 10: The comparative displacement frequency spectra for the two actuation frequencies.

To sum, the half ZGV frequency actuation can be utilized to generate the ZGV mode at the vicinity of damage site, triggering drastic local resonance and thus intense interactions of damage interfaces. Such interactions could largely amplify the nonlinear ultrasonic response against the external disturbances to enhance the performance of nonlinear ultrasonic methodologies.

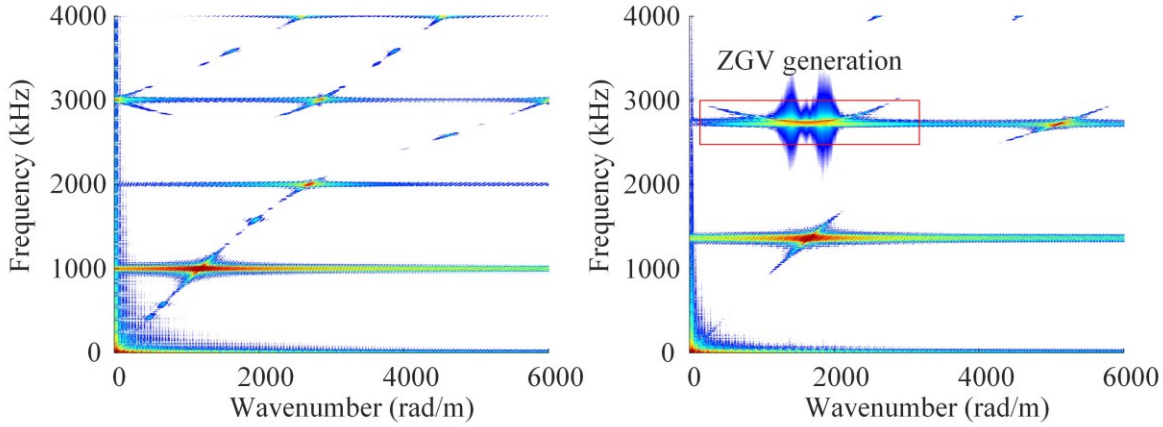

Figure 11: The comparative dispersion curve for the two actuation frequencies.

Summary

This paper proposed the zero group velocity (ZGV) mode enhanced structural health monitoring (SHM) strategies to enhance the performance of EMIS and nonlinear ultrasonics methodologies. From the FE analyses, the distinctive trembling features following ZGV resonances were visualized and validated, and subsequently leveraged for structural sensing of multi-layer laminate. Further, the ZGV resonances were utilized for the amplification of second harmonics generation. It demonstrated that the nonlinear ZGV generation can drastically enlarge the second harmonic component, thus promoting the effectiveness of nonlinear ultrasonics.

Acknowledgement

The support from the National Natural Science Foundation of China (contract number 52475161) is thankfully acknowledged; Funding of John Wu and Jane Sun Endowed Professorship is gratefully acknowledged.

References

[1] C. Prada, D. Clorennec, and D. Royer, "Local vibration of an elastic plate and zero-group velocity Lamb modes," *J Acoust Soc Am,* vol. 124, no. 1, pp. 203-12, Jul 2008, doi: 10.1121/1.2918543.

[2] S. D. Holland and D. E. Chimenti, "Air-coupled acoustic imaging with zero-group-velocity Lamb modes," *Applied Physics Letters,* vol. 83, no. 13, pp. 2704-2706, 2003, doi: 10.1063/1.1613046.

[3] C. Prada, O. Balogun, and T. W. Murray, "Laser-based ultrasonic generation and detection of zero-group velocity Lamb waves in thin plates," *Applied Physics Letters,* vol. 87, p. 194109, November 01, 2005 2005, doi: 10.1063/1.2128063.

[4] C. Prada, O. Balogun, and T. W. Murray, "Laser-based ultrasonic generation and detection of zero-group velocity Lamb waves in thin plates," *Applied Physics Letters,* vol. 87, no. 19, p. 194109, 2005, doi: 10.1063/1.2128063.

[5] D. Clorennec, C. Prada, and D. Royer, "Laser ultrasonic inspection of plates using zero-group velocity lamb modes," *IEEE Transactions on Ultrasonics, Ferroelectrics, and Frequency Control,* vol. 57, no. 5, pp. 1125-1132, 2010, doi: 10.1109/TUFFC.2010.1523.

[6] C. M. Grunsteidl, I. A. Veres, and T. W. Murray, "Experimental and numerical study of the excitability of zero group velocity Lamb waves by laser-ultrasound," *J Acoust Soc Am,* vol. 138, no. 1, pp. 242-50, Jul 2015, doi: 10.1121/1.4922701.

[7] O. Tofeldt and N. Ryden, "Zero-group velocity modes in plates with continuous material variation through the thickness," *J Acoust Soc Am,* vol. 141, no. 5, p. 3302, May 2017, doi: 10.1121/1.4983296.

[8] G. Yan, S. Raetz, N. Chigarev, V. E. Gusev, and V. Tournat, "Characterization of Progressive Fatigue Damage in Solid Plates by Laser Ultrasonic Monitoring of Zero-Group-Velocity Lamb Modes," *Physical Review Applied,* vol. 9, no. 6, 2018, doi: 10.1103/PhysRevApplied.9.061001.

[9] V. Yantchev, L. Arapan, I. Katardjiev, and V. Plessky, "Thin-film zero-group-velocity Lamb wave resonator," *Applied Physics Letters,* vol. 99, no. 3, 2011, doi: 10.1063/1.3614559.

[10] J. Laurent, D. Royer, T. Hussain, F. Ahmad, and C. Prada, "Laser induced zero-group velocity resonances in transversely isotropic cylinder," *J Acoust Soc Am,* vol. 137, no. 6, pp. 3325-34, Jun 2015, doi: 10.1121/1.4921608.

[11] M. Ces, D. Royer, and C. Prada, "Characterization of mechanical properties of a hollow cylinder with zero group velocity Lamb modes," *J Acoust Soc Am,* vol. 132, no. 1, pp. 180-5, Jul 2012, doi: 10.1121/1.4726033.

[12] J. Laurent, D. Royer, and C. Prada, "In-plane backward and zero group velocity guided modes in rigid and soft strips," *J Acoust Soc Am,* vol. 147, no. 2, p. 1302, Feb 2020, doi: 10.1121/10.0000760.

[13] Y.-T. Tsai and J. Zhu, "Simulation and Experiments of Airborne Zero-Group-Velocity Lamb Waves in Concrete Plate," *Journal of Nondestructive Evaluation,* vol. 31, no. 4, pp. 373-382, 2012/12/01 2012, doi: 10.1007/s10921-012-0148-6.

[14] J. Spytek, A. Ziaja-Sujdak, K. Dziedziech, L. Pieczonka, I. Pelivanov, and L. Ambrozinski, "Evaluation of disbonds at various interfaces of adhesively bonded aluminum plates using all-optical excitation and detection of zero-group velocity Lamb waves," *NDT & E International,* vol. 112, 2020, doi: 10.1016/j.ndteint.2020.102249.

[15] Q. Liu *et al.*, "Advancing measurement of zero-group-velocity Lamb waves using PVDF-TrFE transducers: first data and application to in situ health monitoring of multilayer bonded structures," *Structural Health Monitoring,* 2022, doi: 10.1177/14759217221126812.

[16] X. Meng, M. Deng, and W. Li, "Validation of zero-group-velocity feature guided waves in a welded joint," *Ultrasonics,* vol. 136, p. 107173, Jan 2024, doi: 10.1016/j.ultras.2023.107173.

[17] Y. Wu, R. Cui, K. Zhang, X. Zhu, and J. S. Popovics, "On the existence of zero-group velocity modes in free rails: Modeling and experiments," *NDT & E International,* vol. 132, 2022, doi: 10.1016/j.ndteint.2022.102727.

[18] B. Ji, R. R. Mehdi, G.-W. Jang, and S. H. Cho, "Determination of third-order elastic constants using change of cross-sectional resonance frequencies by acoustoelastic effect," *Journal of Applied Physics,* vol. 130, no. 23, p. 235105, 2021, doi: 10.1063/5.0069579.

[19] C. Grunsteidl, T. W. Murray, T. Berer, and I. A. Veres, "Inverse characterization of plates using zero group velocity Lamb modes," *Ultrasonics,* vol. 65, pp. 1-4, Feb 2016, doi: 10.1016/j.ultras.2015.10.015.

[20] D. Clorennec, C. Prada, and D. Royer, "Local and noncontact measurements of bulk acoustic wave velocities in thin isotropic plates and shells using zero group velocity Lamb modes," *Journal of Applied Physics,* vol. 101, no. 3, p. 034908, 2007, doi: 10.1063/1.2434824.
[21] P. Mora, M. Chekroun, S. Raetz, and V. Tournat, "Nonlinear generation of a zero group velocity mode in an elastic plate by non-collinear mixing," *Ultrasonics,* vol. 119, p. 106589, Feb 2022, doi: 10.1016/j.ultras.2021.106589.
[22] W. Li, C. Zhang, and M. Deng, "Modeling and simulation of zero-group velocity combined harmonic generated by guided waves mixing," *Ultrasonics,* vol. 132, p. 106996, Jul 2023, doi: 10.1016/j.ultras.2023.106996.